Defect and Diffusion Forum Vol. 311 (2011) pp 39-61
Online available since 2011/Mar/15 at www.scientific.net

doi:10.4028/www.scientific.net/DDF.311.39

Impurities in Magnetic Materials Studied by PAC Spectroscopy

Artur Wilson Carbonari[a], José Mestnik-Filho[b] and Rajendra Narain Saxena[c]

Instituto de Pesquisas Energéticas e Nucleares, IPEN-CNEN/SP,

05508-000 São Paulo, SP Brazil

[a]carbonar@ipen.br, [b]jmestnik@ipen.br, [c]rnsaxena@ipen.br

Keywords: Magnetic Hyperfine Field, PAC Spectroscopy, Localized Magnetic Moments, Magnetic Materials.

Abstract. Perturbed gamma-gamma angular correlation (PAC) spectroscopy is a precise and highly efficient tool to follow the temperature dependence of local magnetic fields in any material. Its resolution and efficiency does not depend on temperature and therefore can measure local fields at low as well as high temperatures with the same accuracy. Due its versatility in using different probe nuclei it can sense the local magnetic fields at different sites in the crystalline structure of materials. In this review, important results obtained with PAC spectroscopy are shown in two classes of materials: transition metal and transition-metal based compounds and rare earth elements and rare-earth-element based compounds using mainly three different probe nuclei: ^{111}Cd, ^{181}Ta and ^{140}Ce. PAC spectroscopy has contributed to the systematic study of the magnetic hyperfine field in impurities in matrices of Fe, Co and Ni as well as in transition-metal based Heusler alloys. It has also provided important contribution to the investigation of magnetism in rare-earth elements and intermetallic compounds. A still open issue concerning the local fields in metallic magnetic compounds and elements is the exchange interaction between the magnetic ions of the host and a dilute magnetic impurity, which acts as a defect in the magnetic lattice. PAC spectroscopy has been contributing to study this problem with success. Also shown in this review is the crucial role of ab-initio first principle calculations in the interpretation of PAC results.

Introduction

Impurities in magnetic materials play an important role in condensed matter physics because they act as defects in the magnetic lattice that can provoke large effects in the magnetic properties of the materials. In fact, the behavior of such impurities in magnetic materials is essential for a better understanding of magnetism in intermetallic compounds. Also, in order to understand the magnetic behavior of intermetallic compounds where two different magnetic atoms are present it is very important to have a precise description of the exchange interaction between impurity magnetic atoms and magnetic atoms of matrix where these impurities are embedded.

Because of the local character of the magnetic behavior of impurities it is desirable to use a very accurate and sensitive technique such as those based on hyperfine interactions, which can precisely measure the local magnetic field at a probe nucleus substituting a given site in the magnetic crystal. The magnetic hyperfine field (MHF) is sensitive to spin polarization, orbital angular moments of open electronic shells, and magnetic dipole moments, which provide information on the exchange interactions that give origin to several magnetic properties of materials. Particularly the magnetic hyperfine field is sensitive to *s*-polarization what cannot be measured by any other method.

The interaction between a nucleus and electric or magnetic field such as those produced in solids by electrons and other nuclei in the vicinity of the nucleus is called hyperfine interaction. An externally applied magnetic field may also be present. Both electric and magnetic hyperfine interactions may occur. Imagine an atomic nucleus implanted in a ferromagnetic host material. The interaction between nuclear moments and spin polarized electrons in the host lead to an effective field experienced by the nucleus, which is commonly called “hyperfine field”. The hyperfine field provides us with microscopic information on the electronic state of the host and has been

investigated extensively especially in the 3*d* transition ferromagnets such as Fe, Co and Ni [1] and in Gd [2]. A number of techniques, principal among them, perturbed gamma-gamma angular correlation (PAC), perturbed angular distribution of gamma rays (PAD), Mössbauer Effect (ME), and nuclear magnetic resonance (NMR) have been used to obtain a large quantity of experimental data on local magnetism at impurities in magnetic elements as well as in intermetallic compounds. Intermetallic compounds containing rare-earth elements show a large variety of interesting magnetic properties especially when impurities are present. These properties are not well described so far, and techniques that can investigate such properties in an atomic scale are necessary. Among these techniques PAC spectroscopy is one that can provide valuable information on local magnetic field at probe atom sites acting as impurities in magnetic compounds. Although data obtained by PAC measurements are similar to those from classical magnetization measurements, they can provide information on the dynamics of the magnetism near the critical points, on the paramagnetic behavior and the contribution from conduction *s*-electrons. Because PAC does not need an external magnetic field that can affect the spontaneous magnetic mechanism, it can be used to measure magnetic fields in compounds with rare-earth elements which can have a very large neutron absorption cross section making it practically impossible to use neutron scattering techniques.

Due to their large orbital contribution, rare-earth nuclei are not suited to investigate the exchange magnetism between magnetic neighbors in rare-earth based compounds or single elements. Differently from resonance techniques that use the rare-earth itself as probe nuclei and therefore are not able to measure the magnetic contribution due to valence or conduction electrons, PAC permits the study of such materials using the same probe nuclei to measure local magnetic fields in compounds with different rare-earths elements in order to systematically investigate such contributions. Furthermore, the large orbital momentum in rare-earth nuclei opens an opportunity to study the effect of their own orbital angulat momentum on the magnetic hyperfine field in rare-earth compounds, and PAC spectroscopy has explored this fact.

Magnetic hyperfine Interaction

The magnetic nuclear dipole moment $\vec{\mu}$ interacts with the magnetic field $\vec{H}_{hf}$ at the position of the nucleus. The interaction energy is given as

$$E_{mag} = -\vec{\mu} \cdot \vec{H}_{hf} . \quad (1)$$

The interaction energy lifts the degeneracy of the nuclear states and induces the precession of the nuclear spin. Quantization of angular momentum $\vec{I}$, however allows only certain orientations of $\vec{\mu}$ with respect to $\vec{H}_{hf}$. Choosing quantization axis z parallel to $\vec{H}_{hf}$ the interaction energy can be expressed as

$$E_{mag} = -\vec{\mu} \cdot \vec{H}_{hf} = -\gamma \hbar \vec{I} \cdot \vec{H}_{hf} , \quad (2)$$

where $\gamma = \frac{g\mu_N}{\hbar}$, g is the nuclear g-factor, and μ_N the nuclear magneton. The eigenvalues are given as $\mu_N H_{hf} m_I$, where m_I = -I, -I+1, …,I are the projections of the nuclear total angular momentum on the quantization axis. In this manner the magnetic interaction splits the state with spin I into 2I+1 equidistant Zeeman levels. The transition energy between the adjacent levels is $\Delta E = \hbar\omega_L = -g\mu_N H_{hf}$, and the so called Larmor frequency is given as $\omega_L = -\frac{g\mu_N H_{hf}}{\hbar}$.

There are several mechanisms that are responsible for the existence of a magnetic field at the nuclear position. With the exception of an applied external field and disregarding the Lorentz and the demagnetization fields, all these mechanisms have electronic origin. The magnetic hyperfine field can, therefore, be written as a sum of such contributions:

$$\vec{H}_{hf} = \vec{H}_{orb} + \vec{H}_{dip} + \vec{H}_c , \quad (3)$$

where $\vec{H}_{orb}$ is the field produced by the orbital motion of the electrons, $\vec{H}_{dip}$ is the field originated from the distribution of the electronic spins around the nucleus and the Fermi-contact field, $\vec{H}_c$, is the field produced by the difference of the spin-up and spin-down populations of s-electrons at the nuclear position. For the last two of these contributions it is usual to make additional divisions. For example, for the dipolar contribution, $\vec{H}_{dip}$ a distinction is made between the field originated from the electronic spin density of the atom where the nucleus sits and the one that emerges from the summation of the contributions from the magnetic moments of all the other atoms within the material. This last term is sometimes called “lattice contribution".

For the Fermi-contact field $\vec{H}_c$, a first distinction is made for the contributions originated from the core or valence electrons. The core polarization is a manifestation of the change of the shape of *s*-wave functions caused by the presence of a local magnetic moment. The local *s-d* (or *s-f*) exchange interaction pushes the *s*-electrons wave-functions with opposite spin into the nuclear region and pull-out the ones with the same spin polarization. The result is a net s-polarization at the nuclear region that is opposite to that of the local *d* (or *f*) moment. The same effect also happens with the *p* electrons but its result is not visible within the non-relativistic approximations since the *p* wave-functions have zero value at the origin. On the other hand, with relativistic wave-functions, the presence of a small contact field due to *p* wave-functions can also be foreseen.

The valence electrons have also distinct contributions to the Fermi-contact hyperfine field. One of them is the “transferred field" which comes from the hybridization of the impurity valence s-electrons with the neighboring *d*-polarized (or eventually *f*-polarized) atoms. The impurity valence *s*-electrons become polarized by this hybridization and contribute to the Fermi-contact field. The other two contributions have their origin from the effect of its own polarized d-shell of the impurity called “local valence hyperfine field" [3]. The first one is due to the same effect of contracting or expanding the s-wave-function by the local exchange interactions as in the case of core, but in an opposite fashion. The second one, more important, is caused by the same local exchange interaction but produces a re-population of the valence *s*-orbitals since they are not fully occupied as are the core *s*-electrons.

The expressions for the magnetic hyperfine fields which take into account relativistic effects (scalar relativistic approximation) are derived with the recipe outlined in reference 4. The change of the energy due to the interaction of the nuclear magnetic moment with the magnetic moments originated by the electronic spin and orbital angular momentum is given by Blügel et.al. [3] within the scalar relativistic approximation. In the non-relativistic approximation the same can be obtained from Abragam and Bleaney [5]. Since there are some inconsistencies with signs when one compares reference 3 with reference 5, some of the signs from Blügel at.al.[3] were changed. This was done in a way that the magnetic hyperfine fields, in the non-relativistic limit, reduce to the expressions given in reference 5, as it is described below. Then, in reference 3 formulation, the interaction energy for orbital angular momentum and electronic spin are, respectively:

$$\Delta E_{orb} = \frac{e}{mc}\vec{\mu}_I \left\langle \Phi \left| \frac{S(r)}{r^3}\vec{l} \right| \Phi \right\rangle , \quad (4)$$

$$\Delta E_{dip} = \left\langle \Phi \left| \frac{S(r)}{r^3}\left[\vec{\mu}\vec{\mu}_I - 3(\vec{\mu}\hat{r})(\vec{\mu}_I\hat{r})\right] \right| \Phi \right\rangle . \quad (5)$$

In these expressions $\hat{r} = \frac{\vec{r}}{r}$, $\vec{\mu}_I$ and $\vec{\mu}$ are respectively the nuclear and electronic magnetic moments, Φ is the large component of the relativistic wave function, *m*, *e* and *c* are, respectively,

the electron mass, the electron charge and the speed of light, whereas $\vec{l}$ is the one-electron orbital angular momentum operator. *S(r)* is the reciprocal of the relativistic mass enhancement [3]:

$$S(r) = \left[1 + \frac{\epsilon - V(r)}{2mc^2}\right]^{-1}, \tag{6}$$

where ϵ and *V(r)* are, respectively, the total and the potential energy of the electron. Using that $\mu_B = \frac{e\hbar}{2mc}$ and $\vec{\mu} = -2\mu_B\vec{s}$, where $\vec{s}$ is the electron spin, Eq. 4 and Eq. 5 reduce, respectively to:

$$\Delta E_{orb} = 2\vec{\mu}_I\mu_B\left\langle\Phi\left|\frac{S(r)}{r^3}\vec{l}\right|\Phi\right\rangle \quad \text{and} \tag{7}$$

$$\Delta E_{dip} = 2\vec{\mu}_I\mu_B\left\langle\Phi\left|\frac{S(r)}{r^3}\left[3(\vec{s}\hat{r})\hat{r} - \vec{s}\right]\right|\Phi\right\rangle. \tag{8}$$

The change in energy for the contact interaction is:

$$\Delta E_c = \frac{8\pi}{3}\vec{\mu}_I\mu_B\vec{m}_{av}, \tag{9}$$

with, $\vec{m}_{av} = \langle\Phi|\delta_T(r)\vec{\sigma}|\Phi\rangle$, where

$$\delta_T(r) = \frac{1}{4\pi r^2}\frac{\frac{r_T}{2}}{\left[\left(1 + \frac{\epsilon}{2mc^2}\right)r + \frac{r_T}{2}\right]}, \tag{10}$$

$\vec{\sigma}$ are the Pauli matrices, and $r_T = Ze^2/mc^2$ the Thomson radius. Eq. 10 is regarded as a broadened δ-function with a width equal to the Thomsom radius. The Coulomb potential $V(r) = -Ze^2/r$ has been assumed here [3]. Comparing Eq. 7, Eq. 8, and Eq. 9 with the energy of interaction between an external magnetic field with the nuclear magnetic moment, $\Delta E = -\vec{\mu}_I \cdot \vec{H}$, one gets:

$$\vec{H}_{orb} = -2\mu_B\left\langle\Phi\left|\frac{S(r)}{r^3}\vec{l}\right|\Phi\right\rangle, \tag{11}$$

$$\vec{H}_{dip} = -2\mu_B\left\langle\Phi\left|\frac{S(r)}{r^3}\left[3(\vec{s}\hat{r})\hat{r} - \vec{s}\right]\right|\Phi\right\rangle \text{, and} \tag{12}$$

$$\vec{H}_c = -\frac{8\pi}{3}\mu_B\vec{m}_{av}. \tag{13}$$

In the non-relativistic case $S(r) = 1$, $\vec{m}_{av} = 2\vec{s}$, and the corresponding expressions for the fields reduce to the ones given in Ref. 5:

$$\vec{H}_{orb} = -2\mu_B\left\langle\phi\left|\frac{\vec{l}}{r^3}\right|\phi\right\rangle, \tag{14}$$

$$\vec{H}_{dip} = -2\mu_B\left\langle\phi\left|\frac{3\vec{r}\left(\vec{s}\,\vec{r}\right)}{r^5} - \frac{\vec{s}}{r^3}\right|\phi\right\rangle, \text{ and} \tag{15}$$

$$\vec{H}_c = -2\mu_B \frac{8\pi}{3} \left\langle \phi \left| \vec{s}\delta(\vec{r}) \right| \phi \right\rangle, \tag{16}$$

where in this case, $|\phi\rangle$ represents a Schrödinger-type state. In all of the expressions, the magnetic fields are opposite to the angular momenta, as they should be for a negatively charged particle.

The orbital and dipolar fields differ by the factor $S(r)$ when comparing the relativistic with the non-relativistic cases. On the other hand, for the contact field one has to average the electronic magnetization *near* the nuclear position within a region defined by the Thomson radius r_T instead of taking the magnetization *at* the nucleus position. Relativistic wave-functions Φ have to be used instead of the Schrödinger wave-function ϕ in all the cases whenever relativistic effects become important. It is expected that particularly the contact contribution can be very sensitive on the choice of the wave-functions since the relativistic ones have a completely different behavior near the origin (divergent) as compared with the Schrödinger wave-functions [3].

A very useful expression is obtained for the dipolar field if the following equivalence between operators is taken [5]:

$$3\left(\vec{s}\vec{r}\right)\vec{r} - \vec{s} \equiv \frac{2}{(2l+3)(2l-1)}\left[l(l+1)\vec{s} - \frac{3}{2}\left(\vec{l}\cdot\vec{s}\right)\vec{l} - \frac{3}{2}\vec{l}\left(\vec{l}\cdot\vec{s}\right)\right]. \tag{17}$$

Inserting into Eq. 12 and evaluating it for the quantization axis ζ, the dipolar contribution to the magnetic hyperfine field can be finally written as [4],

$$H_\zeta^{dip} = \frac{4\mu_B}{(2l+3)(2l-1)}\left\langle \Phi \left| \frac{S(r)}{r^3}\left\{ l(l+1)s_\zeta - \frac{3}{2}\left[\left(\vec{l}\cdot\vec{s}\right)l_\zeta - l_\zeta\left(\vec{l}\cdot\vec{s}\right)\right]\right\}\right| \Phi \right\rangle, \tag{18}$$

and a very clear dependence of H_ζ^{dip} on a particular (l,m_l,s,m_s) electronic state can be seen. For a given atomic shell composed of several electrons a summation of the fields coming from the individual electronic states of the shell can be performed [3,4] which would then give us the total contribution from that shell.

Magnetism in intermetallic compounds

Intermetallic compounds which present magnetic properties contain two kinds of metallic elements; those with unpaired *f*-electrons and those with unpaired *d*-electrons transition elements. Each of these groups of elements exhibits different properties due to the localized behavior of the unpaired electrons. Whereas the 3*d*-electrons seldom show local moment behavior, the 4*f*-eletrons in most cases present a high degree of localized behavior.

Because of the high delocalization of *d*-electrons the quenching of the orbital angular momentum (L = 0) occurs and, consequently the total angular momentum $J = S$. In this case the energy of the exchange interaction between two unpaired electrons is $V_{exc} = -2J_{exc}\vec{S}_i \cdot \vec{S}_j$ with J_{exc} being the exchange constant, and the energy of the interaction of a localized magnetic moment $\vec{\mu}_i$ due to *d*-electrons with an exchange field is given by

$$E_{exc} = -\vec{\mu}_i \cdot \vec{H}_{exc} = g\mu\vec{S}_i \cdot \vec{H}_{exc}. \tag{19}$$

In magnetic compounds containing rare-earth elements, the magnetism is due to 4f electrons, which are not in the outermost layer of the atom and, consequently are less affected by crystalline field than compounds where 3*d* electrons are responsible for the magnetism. Thus, the energy of the spin-orbit coupling ($\lambda\vec{S}\cdot\vec{L}$) is much greater than the crystal field energy (V_{CEF}) and, therefore, the total angular momentum J of the atom is a good quantum number.

The rare-earth elements are in trivalent state when these are constituents of a compound, with exception of Ce, Eu and Yb that can be in other valence state than 3+. In this trivalent state, the magnetic moment of free rare-earth ions is proportional to $g_J\mu_B\sqrt{J(J+1)}$ in the paramagnetic state and to $g_J\mu_B J$ in the magnetically ordered state. The exchange and crystal field terms are dominant in the total magnetic Hamiltonian for rare-earth ions in a crystal.

Due to the small range of the spatial extension of 4*f* electrons, the magnetism in rare-earth compounds occurs through a mechanism of indirect exchange between the spins of 4*f* electrons. Two mechanisms have then been proposed in which the 4f spins can interact in an indirect coupling. In one of these mechanisms, the coupling between 4f-spins is mediated by means of spin polarization of the *s*-conduction electrons, which occurs by exchange interaction with the 4*f* electrons. The indirect interaction between localized moments was first introduced by Ruderman and Kittel [6] to describe the coupling of nuclear magnetic moments in a metal via hyperfine interaction with conduction electrons. Kasuya[7] and Yosida[8] extended this theory to explain the exchange interaction between localized magnetic moments completing the so-called Ruderman-Kittel-Kasuya-Yosida (RKKY) theory. In the RKKY mechanism, a spin S_i located at a position R_i interacts with the conduction electrons of the metal inducing a spatially non uniform spin polarization given by

$$P(r) = -\frac{9n^2\pi \mathbf{J_{sf}}}{2E_F} S_i F(2k_F r), \tag{20}$$

where E_F and k_F are, respectively the Fermi energy and wave vector, J_{sf} is the effective *s*-*f* exchange constant, and $F(x) = [-x\cos x + \sin x]/x^4$ is the oscillating RKKY function and r is the distance of the conduction electron from the scattering center at R_i. The spin polarization of conduction electrons induced by S_i then interacts with another spin S_j at position R_j with an energy proportional to $\vec{S}_i \cdot \vec{S}_j$:

$$E = \frac{18n^2\pi}{2E_F} \mathbf{J_{sf}^2} \vec{S}_i \cdot \vec{S}_j F(2k_F|R_i - R_j|). \tag{21}$$

As the total angular momentum J rather than the spin S is a good quantum number for rare-earth ions, the spin S is replaced by its projection $(g-1)J$ on the total angular momentum J, and the energy is therefore proportional to $(g-1)^2 J(J+1)$, so that the Curie temperature T_C is proportional to $J_{sf}^2 (g-1)^2 J(J+1)$. In the other indirect coupling mechanism, which was proposed by Campbell [9] the indirect coupling is provided by intra-atomic 4*f* − 5*d* exchange and interatomic 5*d*−5*d* interaction between the spin polarized 5*d* electrons of neighboring rare-earth atoms. As 5*d* electrons are much less localized than the 4*f* electrons of the rare-earth atoms, a considerable overlap occurs between the 5d wave functions of the rare-earth neighbor atoms and, as a consequence a positive direct *d*-*d* interaction is expected. In this mechanism, instead of J_{sf}, an effective *s*-*d* exchange constant J_{sf}, which is a measure of the 4*f*-5*d* exchange interaction, must be used. In contrast, the long range RKKY function also must be replaced by a short-range function that describes the radial dependence of 5*d*-5*d* interaction.

Magnetic hyperfine field measured by PAC spectroscopy

In order to be measured by PAC spectroscopy samples of a magnetic material must have radioactive nuclei incorporated in them. These nuclei must have some convenient properties such as relatively long half-life and must decay to the excited states of the daughter nuclei, hereafter called probe nuclei. The probe nuclei must decay to lower energy states by the emission of two consecutive gamma-rays (γ_1 and γ_2) in a cascade passing through an intermediate level with lifetime long enough to “feel” the hyperfine interaction. The effect of the hyperfine interaction on this

intermediate state lifts the energy degeneracy, splitting it in sublevels. In Table 1 the properties for three probe nuclei commonly used in PAC spectroscopy to measure magnetic hyperfine interactions are shown. PAC spectroscopy measures the hyperfine interaction via the time evolution of the emission pattern of the second gamma-ray (γ_2) in the cascade from a set of nuclei whose intermediate state have been selected by measuring the direction of the first gamma-ray (γ_1).

Table 1: Nuclear properties of three important PAC probe nuclei. $T_{1/2}$ is the half-life of the parent nucleus, E_i is the energy of the intermediate level in the $\gamma_1-\gamma_2$ cascade, I^π and $t_{1/2}$ are the nuclear spin and parity and the half-life of the intermediate level, respectively, and g is the nuclear g-factor.

Parent nucleus	$T_{1/2}$ [d]	Decay mode	Probe nucleus	γ_1 [keV]	γ_2 [keV]	E_i [keV]	I^π	$t_{1/2}$ [ns]	g
^{111}In	2.83	EC	^{111}Cd	171	245	245	$5/2^+$	85	0.306
^{181}Hf	42.4	β^-	^{181}Ta	137	482	482	$5/2^+$	10.8	1.316
^{140}La	1.679	β^-	^{140}Ce	329	487	2083.2	4^+	3.5	1.014

By detecting γ_1, a direction is selected and all nuclei that emitted γ_1 in this direction decay to the same sublevel of the intermediate state. As a consequence, they emit γ_2 with the same emission pattern. If a magnetic field is present the nuclear spin rotates around the direction of the field and, by the angular momentum conservation, the emission pattern rotates as well. PAC measures then the coincidence between the γ_1 and γ_2 signals from two different gamma detectors each one in the same plane by detecting the direction of emission of γ_1 and γ_2 with an angle θ between them. The resulting coincidence function $W(\theta,t)$ gives therefore the probability of coincidence between γ_1 and γ_2 at the angle θ as a function of time between the arrivals of γ_1 and γ_2. The expression for $W(\theta,t)$, neglecting the A_{44} term, is[10]:

$$W(\theta,t) = 1 + A_{22}G_{22}(t)P_2(cos\theta) \tag{22}$$

where A_{22} is the unperturbed angular correlation coefficient of the $\gamma-\gamma$ cascade, $P_2(\cos\theta)$ is the Legendre polynomial, and $G_{22}(t)$ is the perturbation factor that contains detailed information about the hyperfine interaction. In order to obtain the hyperfine interaction, G_{22} must be determined through the measurement of $W(\theta,t)$ by detecting γ_2 in at least two different angles, usually 90º and 180º. Then, the spin rotation function $R(t)$ can be obtained by:

$$R(t) = A_{22}G_{22}(t) = 2\left[\frac{C(180°,t)-C(90°,t)}{C(180°,t)+2C(90°,t)}\right], \tag{23}$$

where $C(\theta,t)$ are the geometric mean of the background subtracted coincidence functions $W(\theta,t)$ recorded at the angle θ. The spin rotation function for an unpolarized magnetic sample is then written as:

$$R(t) = A_{22}G_{22}(t) = A_{22}[0.2 + 0.4cos\omega_L t + 0.4cos2\omega_L t], \tag{24}$$

where ω_L is the Larmor frequency proportional to the magnetic hyperfine field:

$$\omega_L = \frac{g\mu_N}{\hbar}H_{hf}. \tag{25}$$

The sign of the magnetic hyperfine field is also obtained from PAC measurements by applying an external magnetic field perpendicular to the plane of detectors and measuring the ratio $R(t)$ at a fixed angle. $R(t)$ is then expressed in terms of the Larmor frequency, also neglecting A_{44} term, as:

$$R\left(t,\theta=\frac{3\pi}{4}\right)=\frac{N\uparrow-N\downarrow}{N\uparrow+N\downarrow}=-\frac{3}{4}A_{22}\,sin2\,\omega_L t, \tag{26}$$

where N↑ and N↓ are the number of coincidences with applied external field directions up and down, respectively.

The magnetic field at the nucleus of a probe atom is due to unpaired electrons from its partially filled electronic shells. Both spin and orbital motion of such electrons contribute to the magnetic field, as well as exchange interactions between these electrons and electrons from inner filled shells that give rise to the core polarization. When embedded in a magnetic metal, an additional contribution to the magnetic hyperfine field comes from the conduction electrons, which are spin polarized by magnetic ions and induces a contact field at the probe nuclei.

In the case of nonmagnetic probe atoms with filled electron shells, the polarization of conduction electrons (CEP) can be measured by PAC spectroscopy, which is an important tool in the investigation of long-range magnetic interaction between localized magnetic moments in compounds. In this situation, the magnetic hyperfine field is proportional to the net polarization of *s* electrons, given by the difference between spin up and spin down densities at the probe nuclei. A finite *s*-electron spin density may then arise from the spin polarization of the host conduction electrons or by an overlap of the valence electrons of the probe with spin polarized valence electrons of the magnetic atoms.

In intermetallic compounds where the magnetic ion is a 3*d*-transition element the localized magnetic moment can widely vary due to the itinerant character of the 3*d* electrons. In systems such as Heusler alloys where the magnetic atom is Co, for instance, the localized moment at the Co ion (μ_{Co}) can be more than five times greater depending on the other constituent elements.

Heusler alloys are important systems in the study of magnetism due to the possibility to investigate different magnetic phenomena in the same family of alloys. An interesting feature of such alloys is the fact that the magnetic order is strongly dependent upon the state of the chemical order. The X_2YZ Heusler alloys have a cubic $L2_1$ structure consisting of four fcc sublattices, and if one of the X sublattices is unoccupied, the resulting alloy with $C1_b$ structure is called half-Heusler alloy. The potential for technological application of Heusler alloys has enormously increased recently since it was shown that some Heusler alloys either half or full are half metal, where the majority band is semiconducting with a gap at the Fermi level which leads to a full spin polarization. This characteristic makes such alloys good candidates for application in spintronics and spin injection.

PAC spectroscopy was used to investigate the systematic of the hyperfine fields H_{Ta} on ^{181}Ta at Y sites in Co_2YX Heusler alloys[11,12]. The results showed that the values for the reduced fields H_{Ta}/μ_{Co} (μ_{Co} = localized magnetic moment at Co sites) follow the generally observed trend of increasing field with increasing conduction electron density when a group IIIB element Sc at the Y site is replaced by a group IVB element Ti, Zr or Hf with higher number of d-electrons. However, the behavior of V and Nb is anomalous in this respect since the reduced fields decrease when a group IVB element (Ti, Zr or Hf) is replaced in the alloy by a group VB element (V or Nb) with still higher number of *d* electrons, as it is shown in Fig. 1. The explanation for this behavior was given by point-charge model calculations based on RKKY mechanism where the polarization of conduction electrons at a particular probe site due to a magnetic moment located at a distance r_i is given by

$$p(r_i)=\left(\frac{1}{r_i^3}\right)\cos(2k_F r_i+2\delta_0+\eta), \tag{27}$$

where $k_F = 1/a(48\pi^2 n_0)^{1/3}$ is the free-electron Fermi vector given in terms of the average number of conduction electrons n_0 and the lattice parameter a. The term $\delta_o = \pi/4(Z - n_o)$ is the phase shift that takes into account the perturbation of the conduction electron density due to the effective charge Z of the probe atom, and the term η is a pre-asymptotic correction. The hyperfine field at the probe site (impurity) is then expressed as a sum of the contributions to the polarization from the neighboring magnetic moments $\mu(r_i)$:

$$H_{hf} = A\sum_i \mu(r_i)p(r_i), \qquad (28)$$

where A is the hyperfine coupling constant, which has the same value for a given impurity probe atom. As the variation of Z elements in Co_2YZ do not appreciably change H_{hf}, the experimental values of the reduced magnetic hyperfine field as well as the corresponding calculated polarizations were averaged for alloys containing the same Y element but different Z elements and the results are presented in Fig. 2 and show a striking similar behavior.

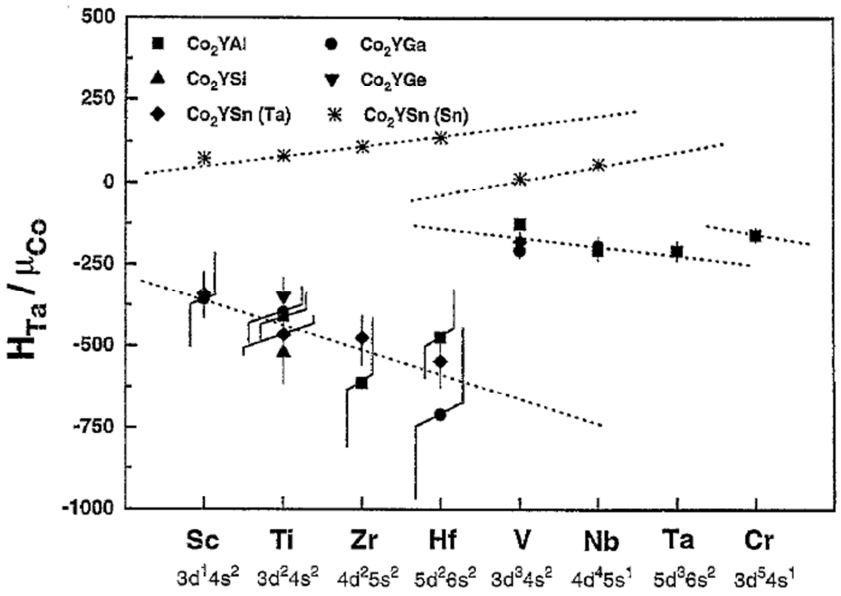

Fig. 1: Reduced magnetic hyperfine field at Y sites in Co_2YZ Heusler alloys measured with PAC spectroscopy using ^{181}Ta as probe nuclei as a function of Y element. [taken from reference 12]

As the conduction electron polarization mechanism is very important in rare-earth compounds, PAC has also given a great contribution to elucidate the coupling mechanism in series of compounds based on rare-earth elements. The magnetism in rare-earth compounds with sp-elements, for instance, Al or In, are supposed to be due to an indirect coupling between two rare-earth ions via s-conduction electron. PAC measurements in R_2In compounds, where R = rare-earth elements[13], using ^{111}Cd as probe nuclei showed, however, that the coupling mechanism between R ions is more likely to be through a direct 5*d*-5*d* interaction than via RKKY polarization. If there is a 4*f*-5*d* exchange in the rare-earth atom, the hyperfine field at the probe is due to an overlap of the spin polarized 5*f* electrons with the valence electrons of the probe atom. Since the 5*d* electrons are much more localized than s electrons, H_{hf} is proportional to the number N of R nearest neighbors and their distance R_i to the probe [13]:

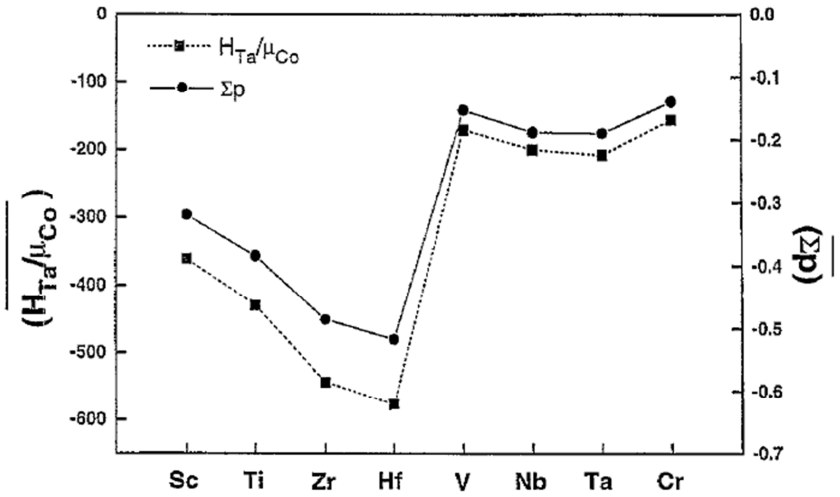

Fig. 2: Experimental values of reduced hyperfine fields compared to the calculated polarization (given by Eq. 27) as a function of Y element in Co_2YZ Heulser alloys. Both values were averaged for alloys containing the same Y but different Z elements. [taken from reference 12]

$$H_{hf} \propto C\Gamma(g-1)J\sum_{i=1}^{N} f(R_i) \quad , \tag{29}$$

where $f(R_i)$ accounts for the contribution of each R nearest neighbor to H_{hf}. In R_2In compounds, the probe atom has 11 nearest R neighbor at a slightly smaller average distance than that of the 12 nearest neighbor in R metals. Therefore, if H_{hf} is proportional to the number of R nearest neighbor it is expected that the ratio $H_{hf}(R_2In)/H_{hf}(R) = 11/12 = 0.92$. On the other hand, if it is assumed that the RKKY is the coupling mechanism for the R atoms, the ratio $H_{hf}(R_2In)/H_{hf}(R)$ is expected to be around 0.6. The experimental ratio for MHF measured with ^{111}Cd is $H_{hf}(R_2In)/H_{hf}(R) \approx 0.9 – 1.1$[13] which implies that the coupling mechanism between neighbor R atoms is through 4*f*–5*d* exchange followed by direct 5*d*–5*d* interaction.

The use of magnetic rare-earth probe nuclei in hyperfine interaction techniques introduces a contribution from the probe itself to the measured magnetic field, $H_{hf} = H_{4f} + H_{core}$, where H_{4f} is the magnetic field from the 4*f* moment and H_{core} is the contact field from the *s*-electrons in the core polarized by the 4*f* moment. In the Lanthanide series Ce^{3+} is the first ion, which has only one *f* electron. As this *f* electron is not as localized as *f* electrons in other rare-earth ions, Ce is an important probe to sense local magnetic field at rare-earth sites as well as to study the contribution of the single 4*f* electron to the magnetic hyperfine field. Because Ce ion has only one 4*f* electron in the Ce^{3+} state, and none in the Ce^{4+} state, it can sometimes display a mixed valence state.

Although being a rare-earth element, ^{140}Ce when embedded in a crystal can be in 4+ state which means that the 4*f* layer is empty and the probe atom has closed shell configuration. In this situation this probe can sense the conduction electron polarization and give information about the polarization at a rare-earth atomic site in compounds where one of the constituent elements is a rare-earth atom. This is the case in a PAC spectroscopy study of ferromagnetic compounds RNiIn, where R = Gd, Tb, Dy, Ho are heavy rare-earths, using ^{140}Ce and ^{111}Cd as probe nuclei [14, 15]. In these compounds, ^{140}Ce substituted R atoms whereas ^{111}Cd substituted In atoms, and it was possible to compare the MHF at two different sites in the compounds.

The results of the temperature dependence of the magnetic hyperfine field $H_{hf}(T)$ for each compound show that the temperature T above which the $H_{hf}(T)$ is zero is different for ^{140}Ce (T_{Ce}) and ^{111}Cd (T_{Cd}), as shown in Fig. 3. The temperature T_{Ce} agrees with T_C obtained by magnetization

measurements, and it is higher than T_{Cd} for each compound. Interestingly, the difference $T_{Ce} - T_{Cd}$ increases as T_C increase, as shown in Fig. 4.

The difference in the temperatures at which H_{hf} is zero for ^{140}Ce probe at *R* sites and ^{111}Cd probe at In sites in each compound was explained by the difference in the local neighborhood of each site and crystal field effects. The crystal structure of *R*NiIn compounds is built out of two types of basal plane layers one with (3*R*+Ni) for $z = 0.5$ and another without rare-earth atoms (3In +2Ni) for $z = 0$. The exchange interaction that gives rise to magnetism in these compounds is larger within the atomic planes than the interaction between the planes. This explains the relative independence of the two magnetic systems in the same compound.

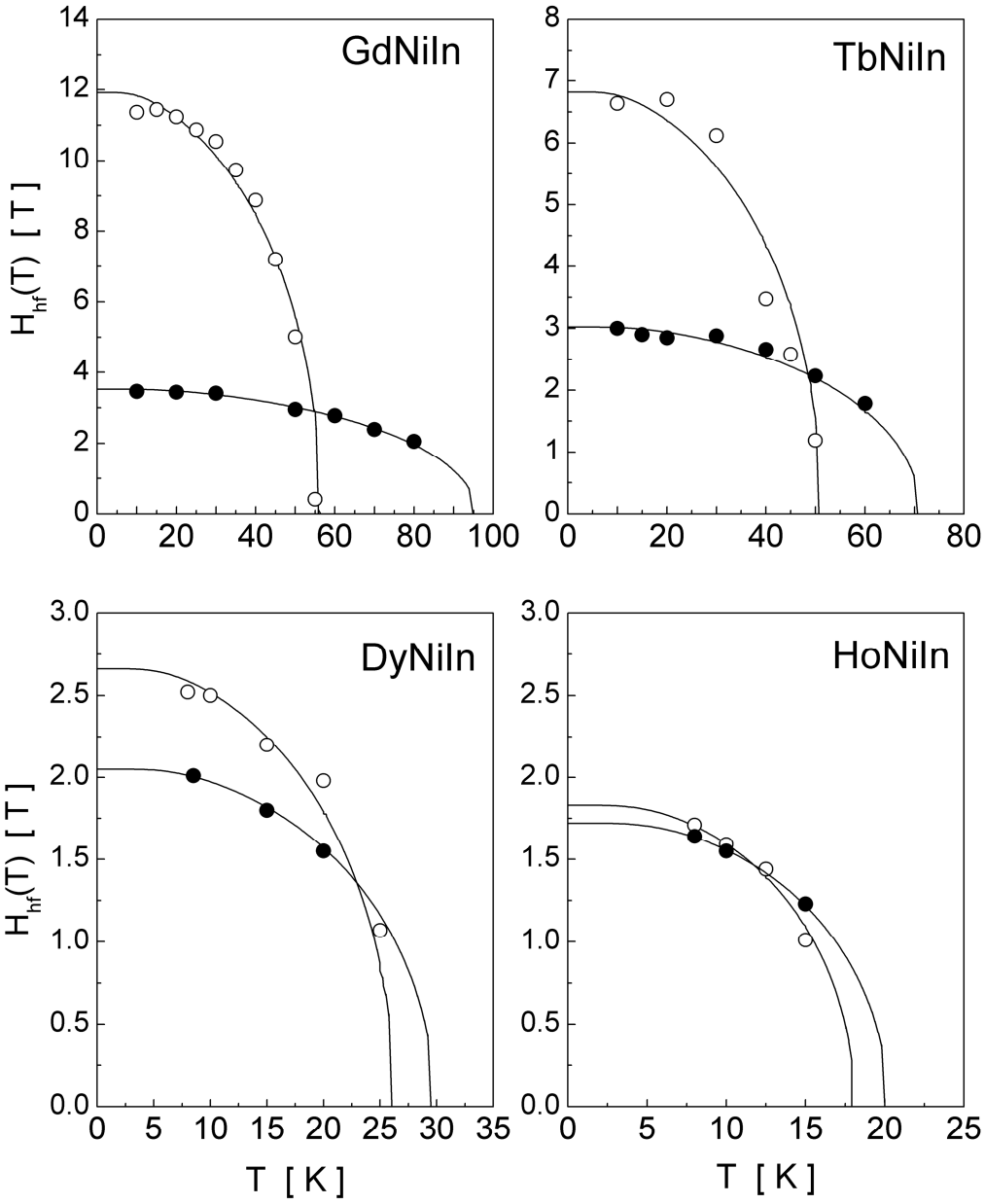

Fig. 3: Temperature dependence of H_{hf} in RNiIn at In sites (open circles) measured with ^{111}Cd, and at Ce sites (full circles) measured with ^{140}Ce. [taken from Ref. 14]

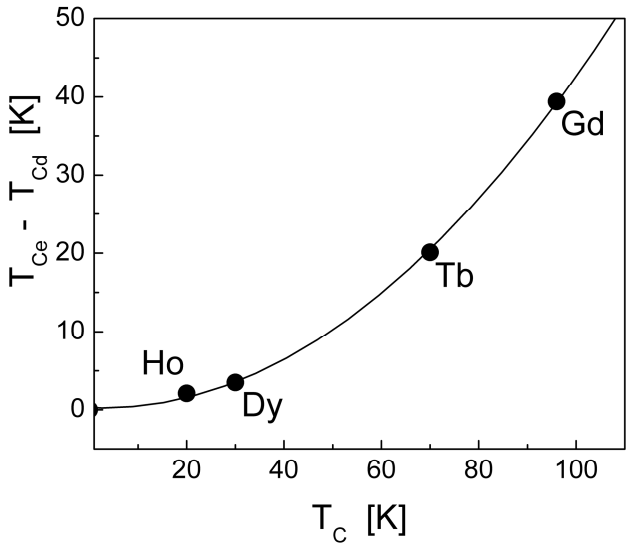

Fig. 4: Difference in the magnetic ordering temperatures observed with PAC measurements using ^{140}Ce (T_{Ce}) and ^{111}Cd (T_{Cd}) in RNiIn compounds as a function of the Curie temperature of each compound. [taken from Ref. 14]

Electronic structure calculations

The magnetic hyperfine fields are extremely sensitive to the electronic structure of the atom at which the fields are determined and consequently to the electronic structure of the whole material under observation. Due to this fact, to correctly interpret the results of an experiment such as PAC measurements, very precise information on the electronic structure of a material is needed. Conversely, when a good agreement between a measured MHF with a calculated one is established without ambiguities, it can be said that the electronic structure of the material is known with great accuracy. Because of the advent of the new powerful computational techniques, new theoretical developments and a continuous decrease of computers prices, several laboratories which were engaged only on experimental activities began to perform theoretical electronic computations as well within the last decade. Electronic structure calculations are nowadays widely spread mainly because of the simplification (and consequently large gain in computational speed) of the electronic interactions problem after the rigorous establishment of the basis of the “Density Functional Theory" in 1964-65 by Hohenberg, Kohn and Sham [16, 17].

In essence, the statement of the electronic structure problem is very simple. In its simplest form, the Hamiltonian of the problem establish nothing more than the several possible Coulomb interactions between particles within a solid, namely, nuclei-nuclei, nuclei-electrons and electrons-electrons with the addition of the kinetic energies of these particles. The Born-Openheimer approximation is then applied by which the nuclear degrees of freedom are detached from the electronic ones reducing the problem to another equivalent one where interactions between nuclei do not exist anymore but the electrons sense an affective “external" potential from the frozen nuclei. Even with this approximation, the problem still demands unpractically large efforts to be solved. What makes this problem intractable from the computational point of view, i.e., to obtain a solution with all the eigenvalues and eigenvectors, is the term due to the interaction between the electrons.

Within the density functional theory (DFT) the problem is totally re-stated. Instead of wave-functions, the method employs the electronic density $\rho(r)$ or, within a more sophisticated approach,

the spin densities $(\rho_{\uparrow}, \rho_{\downarrow})$. This charge or spin density is constructed by "pseudo" non-interacting particles. The problem is thus transformed from a system of *n* interacting particles into an equivalent problem with *n* single-particle systems but, they are now under the influence of an additional and unknown exchange and correlation potential V_{xc}, *n* being the number of electrons of the system. All the observables are now functionals of the density, $\langle \hat{O} \rangle = O(\rho)$ and the method allows one to obtain the ground-state density of the system (only the ground-state) with the aid of the Rayleigh-Ritz variational principle once an approximation for the unknown exchange-correlation potential $V_{xc}(\rho)$ is provided. Details of this method can be seen in [18-20] and the references therein.

Magnetic Hyperfine fields at cerium atoms

Cerium compounds and materials containing cerium as impurities belong to a particular family of systems that present a large variety of phenomena such as magnetism, Kondo effect, superconductivity, intermediate valence, heavy fermions behavior, among others, leading to a special interest of the researchers. Several of these phenomena have straight relationship with the role that Ce-4*f* electrons play and the corresponding electronic states that they can adopt.

The perturbed angular correlation community has also a particular interest in cerium compounds due to the possibility to measure magnetic hyperfine fields at the cerium nuclei employing the $^{140}La \rightarrow ^{140}Ce$ probe produced by the bombardment of ^{139}La with neutrons in a nuclear reactor. Magnetic hyperfine fields measured at Ce nucleus have sometimes a large contribution from its orbital electronic 4*f* state but it is also common that this contribution has the same order of magnitude as the Fermi-contact field, preventing one to determine the origin of the MHF without ambiguity. Complementing the measurements with electronic structure computations not only allows the determination of the several components of the fields but can also give us an insight as to which electronic state is responsible for the measured field.

Several works at our group have been performed with this objective and indeed continues to be an important field of research. One good example is taken from MHF results for the $CeMn_2Ge_2$ compound obtained from PAC experiment [21], and first-principles calculations [22]. PAC results using ^{140}Ce showed that the hyperfine field at Ce atoms in $CeMn_2Ge_2$ does not follow a Brillouin-like behavior as a function of temperature as the field at the Mn sites does. Instead it strongly departs from this behavior, as can be seen in Fig. 5, increasing as the temperature decreases. Besides this, it has a relatively large value of 40 T at 10 K [21], an intriguing result since it was known from neutron diffraction measurements that the Ce atoms in $CeMn_2Ge_2$ do not have a measurable magnetic moment. Carrying on electronic structure calculations for this system [22] it was found that the Ce atoms are indeed magnetic but the spin and orbital magnetic moments nearly cancel each other but the magnetic hyperfine field does not.

Another example of good information extracted from PAC experiment and first-principles calculations for the magnetic hyperfine field can be found in an investigation of $CeIn_3$ compound [23, 24]. Here it is shown how calculations can provide information about the several contributions to the MHF acting on Ce atoms. It was found that in this case the MHF is dominated by the orbital field. The dipolar contribution is negligible due to the anti-ferromagnetic ordering of the Ce atoms and the Fermi-contact field is small due to the almost cancellation of the core and valence contributions. More importantly, calculations have shown that the In atoms in $CeIn_3$ compound have a small MHF, as observed experimentally. This field comes from a small polarization of the In *p*-electrons [24].

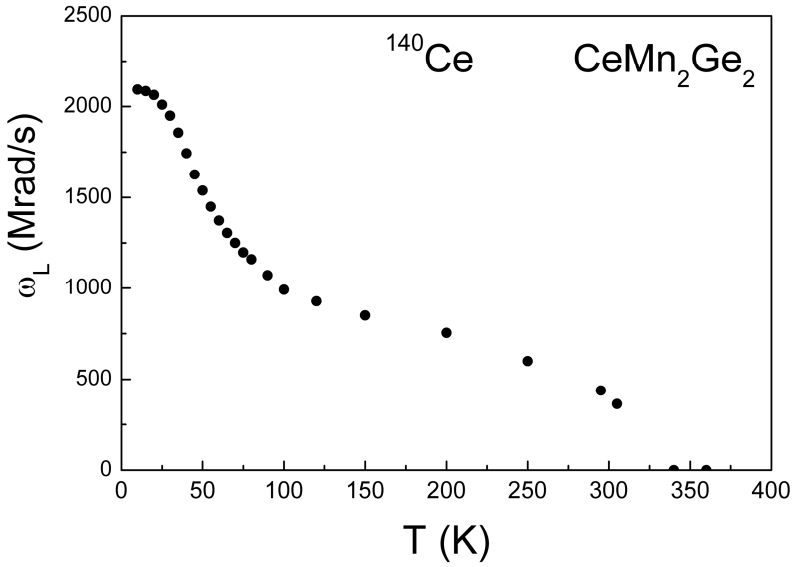

Fig. 5: Temperature dependence of dipole magnetic frequency (ω_L) measured with PAC using ^{140}Ce as probe nuclei. [taken from Ref. 21]

Work done on the measurements and calculations of magnetic hyperfine fields at impurity elements in ferromagnetic matrices can also be found. In fact, for impurities in the Fe matrix, all the elements of the periodic table were studied and the corresponding hyperfine fields theoretically interpreted in a way that the observed systematic trends are now well known. An overview of these studies can be found in Ref. [25, 26]. In the case of 3*d* and 4*d* impurities in Ni one can refer to [3].

When studies of electronic structure of rare-earth elements are performed, a special treatment of their 4*f* shell is needed that go beyond the standard DFT theory because of the large correlation energy involved with these electronic states. This treatment is known as LDA+U approximation and works for the majority of the rare-earth elements are given in [25]. The results however fail sometimes for the lighter rare-earths, Ce being a particular case. This happens because lighter rare-earth elements have more extended 4*f* wave-functions than those in heavier elements that makes them interact to a larger extent with the neighboring electrons. We call these states as being more "de-localized". A very interesting example of this effect can be seen in the Ref. [27]. The Ce atoms as impurities within Co or Gd matrices present very similar MHF in both the situations but the origin of the MHF is completely different. For Ce in Gd the orbital field is large whereas for the Ce in Co case, Fermi-contact field dominates almost exclusively due to the Ce valence electrons. This happens because the Ce atoms being closer to the Co atoms in this case, a pronounced de-localization of the Ce-4*f* occurs that quenches the local magnetic 4*f* moment. With an absent local magnetic moment no core polarization occurs. The valence contribution to the MHF comes from the hybridization with the neighboring polarized Co-3*d* electrons, or, the transferred field.

Another interesting and challenging problem is the interpretation of the temperature dependence of the MHF from Ce atoms in both the situations where they make part of an alloy or when they are impurities. Several works performed so far indicate a behavior that is intrinsic to the Ce MHF. It is seen as an increase of the MHF as the temperature decreases, suggesting that an ordering of the Ce-4*f* states takes place at low temperatures. This behavior was interpreted with a molecular field model in which, as described in details in the next section, it is assumed that the Ce-4*f* state is polarized by means of an exchange interaction with neighboring magnetic atoms and thus depends on the magnetization of the sample. A different exchange interaction constant is assumed between the impurity-host atoms as compared to the host-host exchange interaction energy. It is possible that another mechanism can also be responsible for this effect, namely, transitions of the Ce-4*f* states between crystalline-field states. Work on the search for this kind of mechanism is now in progress.

Dilute magnetic ions in magnetic hosts

An important defect type in magnetic materials that has straight technological applications is the problem of very low concentration (diluted) of magnetic impurities, which posses local moments, in magnetic hosts. This problem is far from being well understood so far. Localized magnetic moments are known to exist on paramagnetic ions, on rare-earth atoms in metals, and on 3d atoms in nonmagnetic hosts. The interpretation is straightforward for all these cases. Localized moments occurring on 3d ions in nonmagnetic metals is due to the degenerate d electrons on the impurity. In the model for localized moments proposed by Anderson [28], the 3d ion is represented by an up- and a down-spin state available for electrons. This ion interacts with the d-band of the host metal and able to absorb and emit electrons. However, for magnetic impurities in magnetic hosts the situation is much more complex.

In a study of dilute Mn in iron matrix, Koi et al. [29] carried out experimental measurements of NMR frequency in 1.5% Mn in Fe matrix using ^{55}Mn as probe atom and the results for the temperature dependence of the NMR frequency ν_T showed a sharp deviation from the Brillouin-like curve. The interpretation of this data was given first by Jaccarino et. al. [30] who considered a localized moment on Mn atoms and proposed a simple model based on the molecular field calculations in which the magnetic coupling between Mn and Fe atoms is weaker than the magnetic coupling between two Fe atoms. In this model it was assumed, firstly that the NMR frequency ν_T is proportional to the thermal average of the Mn moment $\langle S \rangle_T = SB_S(y)$, where $B_S(y)$ is the Brillouin function with

$$y = \frac{g\mu_B H_{exc}}{KT}, \tag{30}$$

and the magnitude of S is independent of temperature. The thermal average of S is taken over its levels in the exchange field of iron, which scales to the iron magnetization σ_T / σ_o by a constant factor ξ which assumes that the intensity of the host-impurity exchange interaction is different from that of the host-host interaction [30]:

$$H_{exc} = \frac{KT_C}{g\mu_B}\xi\left(\frac{\sigma_T}{\sigma_0}\right). \tag{31}$$

The results for the fitting of $B_S(y)$ to experimental data ν_T / ν_o together with the magnetization σ_T / σ_o are shown in Fig. 6, and the best fit was found when S = 3/2 or S = 1. Low [31] however pointed out that such a large spin of the Mn atom does not agree with results of magnetic moment distribution in FeMn alloy measured by neutron scattering which found that the Mn moment would be around $0.5\mu_B$. In order to improve the model Low [31] suggested adding a term to the calculation of the hyperfine field that takes account of the conduction electron polarization. Shirley et. al. [32] following Low´s suggestion proposed a model to calculate the magnetic hyperfine field measured by probe nuclei of magnetic atoms embedded in a magnetic host. In this model the magnetic hyperfine field H_{hf}(T) is the result of the addition of two contributions: one from conduction electrons H_c(T) and another from localized moments in the probe atom H_L(T). The conduction electron contributions is expected to follow the host magnetization so that,

$$H_{hf}(T) = H_c(0)\frac{\sigma_T}{\sigma_0} + H_L(0)B_J(y), \tag{32}$$

where J depends on the crystal field strength, for rare-earth probe atoms which are weakly affected by the crystal field, J is the total angular momentum. Defining $f = H_L(0)/H_{hf}(0)$ as the fraction of $H_{hf}(0)$ that comes from the probe atom contribution, the expression for the magnetic hyperfine field is given by [32]:

$$H_{hf}(T) = H_{hf}(0)\left[fB_J(y) + \frac{(1-f)\sigma_T}{\sigma_0}\right]. \quad (33)$$

This model was then used to analyze H_{hf}(T) data obtained by PAC spectroscopy measurements on ^{99}Ru nuclei that substitute about 1% atomic of Ni. The results for the temperature dependence of the reduced H_{hf}(T) indicate that a localized moment of approximately $0.5\mu_B$ was determined for Ru in Ni [32].

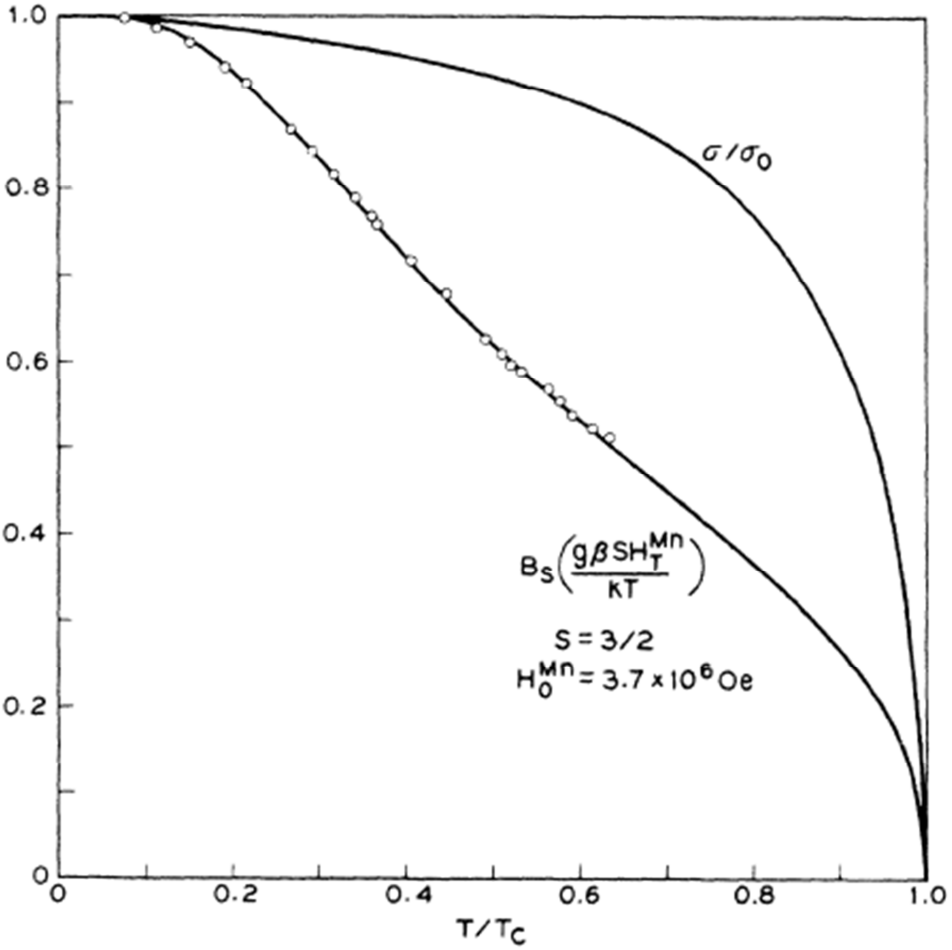

Fig. 6: Reduced NMR frequency ν_T / ν_o (open circles) as a function of the reduced temperature T/T$_C$ for ^{55}Mn at Mn impurities in ferromagnetic iron. The continuous line is the result of the fitting for the Brillouin function using the model described by Eq. 30 and Eq. 31. The reduced magnetization σ_T / σ_o is also shown. [30] [Reprinted with permission from V. Jaccarino, L. R. Walker and G. K. Wertheim: Phys. Rev. Lett. 13, 752 (1964). Copyright 1964 by the American Physical Society]

Although this molecular field model can qualitatively make a good interpretation of data it, gives quite imprecise quantitative results especially for J and f parameters. In an attempt to provide a more precise calculation of the temperature dependence of H_{hf}(T) at magnetic impurities in magnetic hosts, Campbell [33] reported a model based on Friedel's description[34] of transition metal impurities in ferromagnetic metals in which a screening charge appears around the local potential on the itinerant electrons due to an impurity with effective charge difference with respect to the host. In this model the temperature behavior of H_{hf} is associated with a narrow bound state at the Fermi energy. For a given ferromagnetic host, there is a critical impurity charge difference Z_c for which the total moment per impurity shows an abrupt change when the impurity charge difference Z_i moves along the transition element impurity series. The models predicts an expected

temperature-sensitive behavior for impurities close to Z_c, where the bound state is quite close to the Fermi level, and a behavior insensitive to temperature for very well localized ($Z_i < Z_c$) or very badly localized ($Z_i > Z_c$) impurities.

In the model, for impurities near Z_c existence a high moment state is assumed in which the reduced hyperfine field is $\alpha = (H_{hf} / \sigma)_h$ and a low moment state characterized by $\beta = (H_{hf} / \sigma)_l$, and the relative energies of these states can vary with temperature, $E_h - E_l = E_0 - \lambda T$, with E_0 and λ being parameters to be determined from experiment. The temperature behavior of the hyperfine field at the impurity is given by [33]:

$$H_{hf}(T) = \frac{H_{hf}(0)\sigma_T}{\sigma_0}\left[\frac{1 + \gamma\eta exp\left(-\frac{E_0}{kT}\right)}{1 + \eta \exp\left(-\frac{E_0}{kT}\right)}\right], \quad (34)$$

where $\gamma = \beta / \alpha$ and $\eta = \exp(\lambda / k)$. This model was then used to fit the temperature dependence of ^{55}Mn impurity in Fe [29] and ^{99}Ru impurity in Ni [32] as well as the PAC data for Os in Fe [35] which showed instead of an expected decrease, an increase in the $H_{hf}(T)$ with the increasing temperature.

The molecular field model was extended to rare-earth impurities first by Bernas and Gabriel[36] to explain the results of Integral perturbed angular correlation (IPAC) measurements of the magnetic hyperfine field at ^{169}Tm impurities in iron. In this model the interaction $\mathcal{H}_{sf}$ between a rare-earth spin and conduction electrons is described by introducing an exchange interaction $\vec{H}_{exc}$ so that $\mathcal{H}_{sf} = \mu_B \vec{S} \cdot \vec{H}_{exc} = \mu_B (g_J - 1)\vec{J} \cdot \vec{H}_{exc}$ where the projection of S on J it is used. It was assumed that the ground state of Tm is only split by the exchange interaction from Fe host which is weaker than that between two host Fe ions, and the localized spin is aligned by H_{exc}, which is proportional to the Fe magnetization. Thus, the magnetic hyperfine field at the rare-earth probe nuclei is

$$H_{hf}(T) = H_{hf}(0) B_J\left[\mu_B (g_J - 1)\vec{J} \cdot \frac{\vec{H}^T_{exc}}{kT}\right], \quad (35)$$

where $H^T_{exc} = H_{exc}\left(\frac{\sigma_T}{\sigma_0}\right)$ and H_{exc} must be determined from the experimental data. The result for the temperature dependence of $H_{hf}(T)$ normalized to $H_{hf}(0)$ = 5.6 MOe is shown in Fig. 7.

One interesting probe nucleus is ^{140}Ce because Ce ion can be in 3+ or 4+ valence states possessing only one 4*f* electron or no 4*f* electron, respectively. Therefore, depending on the situation, Ce probe can have a localized moment or not. ^{140}Ce is a PAC probe nucleus and it has been used to measure hyperfine fields in magnetic compounds with rare-earth as a constituent atom. Thiel et al. measured the magnetic hyperfine field in Gd [37] and Tb [38] through PAC spectroscopy using ^{140}Ce as probe nuclei. In order to explain the experimental data for Tb a model was proposed in which the exchange field is

$$H_{exc}(T) = \frac{3kT_C}{(J_h + 1)g_J^h \mu_B}\left(\frac{\sigma_T}{\sigma_0}\right), \quad (36)$$

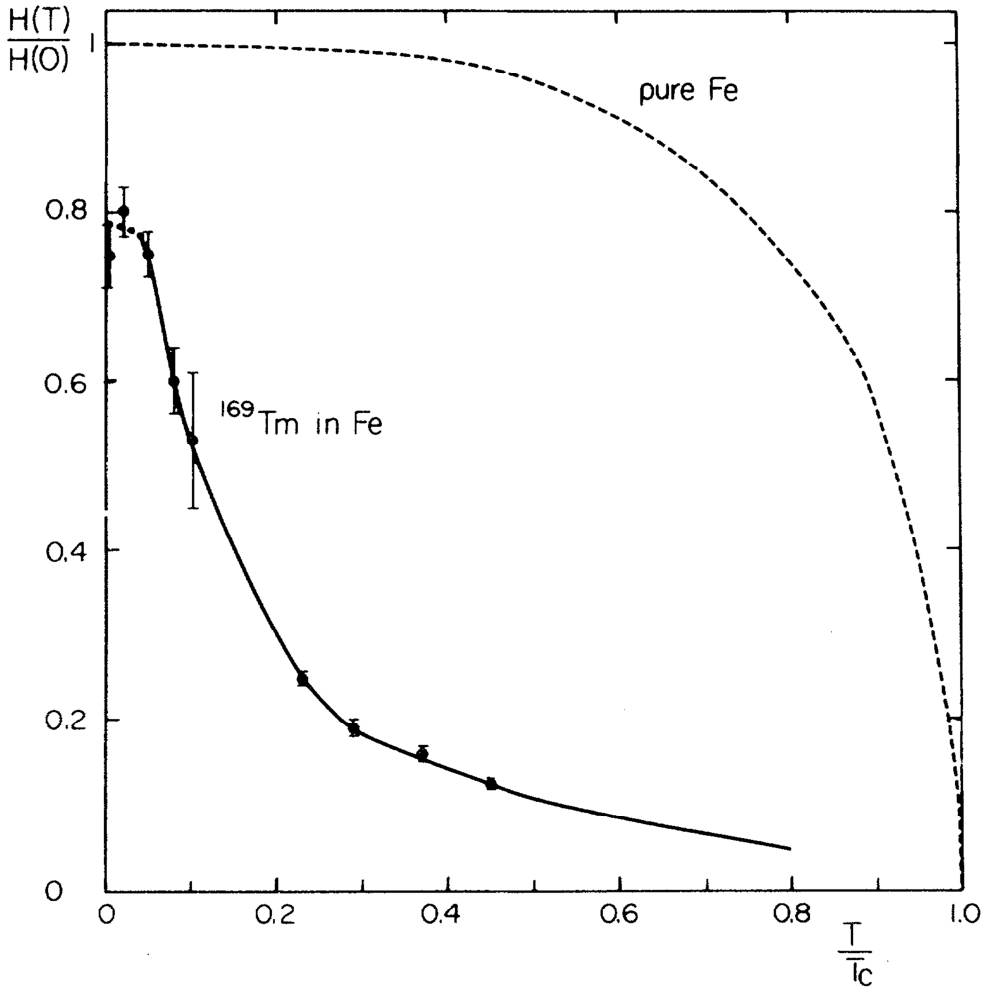

Fig. 7: Reduced magnetic hyperfine field H(T)/H(0) as a function of T/T_C measured at ^{169}Tm in Fe. The continuous line represents the fitting using the molecular field model with the exchange interaction given by Eq. 35. The dotted line is the reduced magnetization for pure Fe. [36] [Reprinted with permission from H. Bernas and H. Gabriel: Phys. Rev. B7, 468 (1973). Copyright 1973 by the American Physical Society.]

where J_h and g_j^h are the total angular momentum and the g-factor of the rare-earth host. In this model it is also assumed that the host-impurity exchange interaction may be different from the host-host exchange interaction by introducing a constant ξ. The model further assumes that the ground state of the magnetic impurity (Ce^{3+}) is only split by the exchange interaction from the rare-earth host, as a consequence the energy of the magnetic sublevel M is

$$E(M,T) = -\mu_B g_j^i J_i H_{exc}(T) = -M g_j^i \frac{3kT_C}{(J_h+1)g_j^h}\xi\left(\frac{\sigma_T}{\sigma_0}\right) + \Delta \quad , \tag{37}$$

where J_i and g_j^i are the total angular momentum and the g-factor of the impurity and Δ is the difference in energy of the multiplet relative to the energy of the impurity when it is nonmagnetic (Ce^{4+}). A magnetic hyperfine field is associated to each sublevel and a contribution from conduction electrons is associated to the nonmagnetic energy. The experimental results for the magnetic hyperfine field at ^{140}Ce in Tb were fitted by the model and the fitting yields ξ = 0.457(9) for the host-impurity exchange parameter.

The model proposed by Thiel et al. was criticized by Wäckelgard et. al [39] who pointed out first, the fact that crystal-field effects was not taken into account in their model, and second, the authors did not use the correct projection of S on J characterized by the factor $g_J - 1$, which, in the case of ^{140}Ce would give a negative contribution to the magnetic hyperfine field. Wäckelgard et. al [39] then proposed to substitute the exchange interaction by

$$H_{exc}(T) = \frac{3kT_C}{2(J_h + 1)\left(g_j^h - 1\right)\mu_B}\left(\frac{\sigma_T}{\sigma_0}\right), \quad (38)$$

which was used to fit PAC results for the magnetic hyperfine field at ^{140}Ce in $CeAl_2$, $GdAl_2$ and $DyAl_2$. In these calculations the effect of crystal-field on the sublevels of Ce^{3+} was also taken into account.

Although the molecular field models have successfully described data on magnetic hyperfine field at magnetic impurities in magnetic hosts, some questions still need to be answered concerning the impurity-host exchange interaction. Is the intensity of this interaction the same for a certain probe atom for different rare-earth elements? Or, is this interaction dependent on the magnetic host?

In order to answer these questions it is firstly necessary to elaborate a reliable model from which it is possible to obtain comparable data. Secondly, it is fundamental to carry out new experiments in order to obtain a systematic set of data in which the same probe atom is used in magnetic host with the same structure but different magnetic constituent atoms.

In an attempt to answer part of the raised questions above, a series of experiments have been carried out using ^{140}Ce as probe nuclei in binary compounds RX where rare-earth R elements are present and X is a transition element from IB or IIB group. These compounds have a simple CsCl-type cubic structure which allows a closer insight in to the 4*f* magnetism. DyAg and DyCu [40], as well as NdAg [41] were investigated by PAC spectroscopy using ^{140}Ce as probe nuclei. As can be seen in Fig. 8 and Fig. 9 the temperature dependence of the magnetic hyperfine field for each compound is far from the expected behavior described by the Brillouin function. In order to describe such behavior the model based on molecular field theory described above was used to fit the experimental data. For the antiferromagnetic Dy compounds, the fitting showed that the exchange interaction between the localized spin in Ce probe and Dy atom is greater in DyCu than in DyAg and the field due to conduction electron polarization H_c is 5.4 T for DyAg and 5.8 T for DyCu at T = 0 K, which yield a ratio $H_c(0)/T_C$ of 0.0952 for DyAg and 0.0954 for DyCu confirming the RKKY prediction that T_C is proportional to the conduction electron polarization.

The compounds in the family RAg (R = rare-earth element) where R ranges from Nd to Tm order anti-ferromagnetically whereas CeAg and PrAg show ferromagnetic ordering. Nd is the next element to Pr in the lanthanide series and NdAg is the first compound in the RAg family that presents anti-ferromagnetic order. The magnetization results for the NdAg sample doped with radioactive ^{140}La, used for PAC measurements, showed a ferromagnetic behavior. The results for the molecular field model fitting to the experimental data yielded a conduction electron contribution ($H_c(0)$ = 23 T) to the magnetic hyperfine field measured for NdAg much higher than that obtained for antiferromagnetic DyAg ($H_c(0)$ = 5.4 T). These results are a strong indication that NdAg ordered ferromagnetically, and, therefore the antiferromagnetic order is unstable if there is an impurity at the Nd sites which acts as a defect in the magnetic lattice as observed in the sample used for PAC measurements, which was prepared with ^{140}La(^{140}Ce) substituting about 0.2% of Nd atoms. In order to investigate whether the magnetic order in NdAg is unstable, *ab-initio* electronic structure calculations on NdAg were carried out in both the ferro and anti-ferromagnetic states of NdAg using a 2x2x1 supercell and a regular 1x1x1 cell for the anti-ferromagnetic and ferromagnetic cases, respectively with the purpose to theoretically determine the difference between the energies of the ferromagnetic and anti-ferromagnetic phases of the NdAg compound.

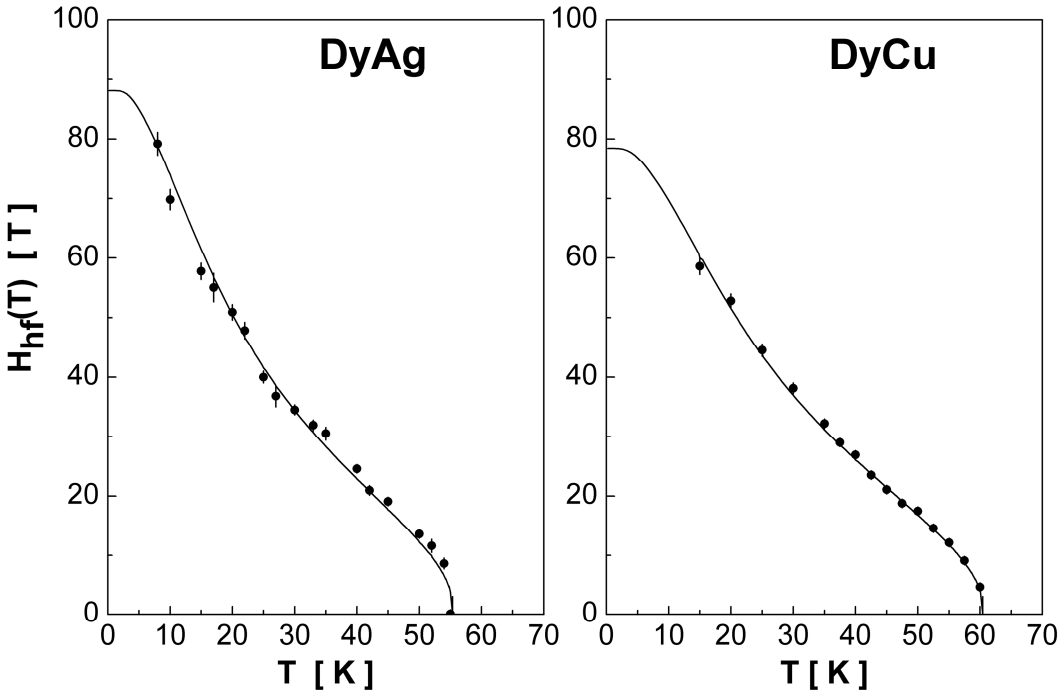

Fig. 8: Temperature dependence of Hhf measured with PAC at ^{140}Ce in DyAg (left) and DyCu (right). The continuous lines are the fitting of data to the model using Eq. 38. [taken from Ref. 40]

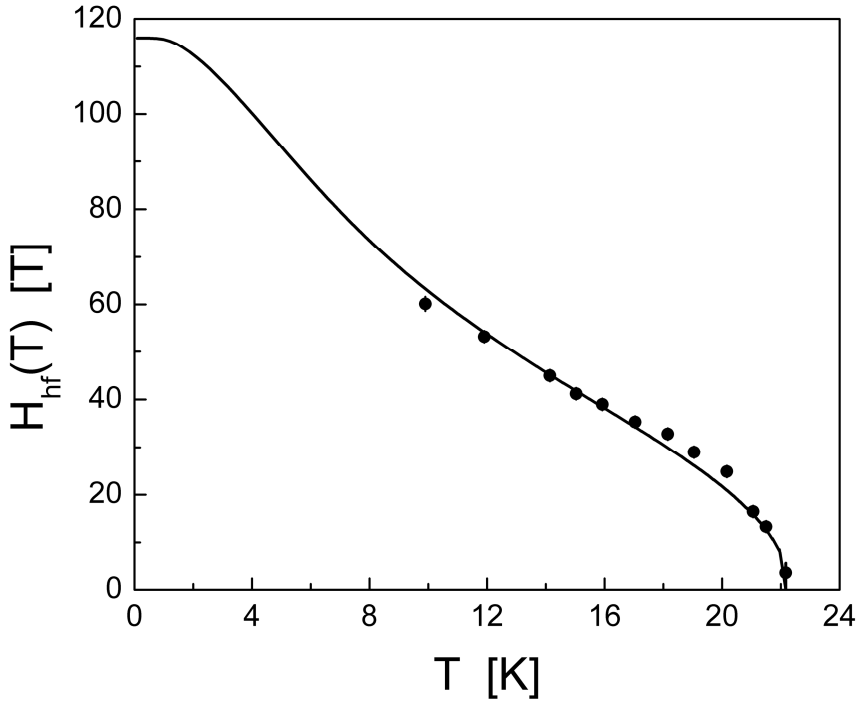

Fig. 9: Temperature dependence of H_{hf} measured with PAC at ^{140}Ce in NdAg. The continuous lines are the fitting of data to the model using Eq. 38. [taken from Ref. 41]

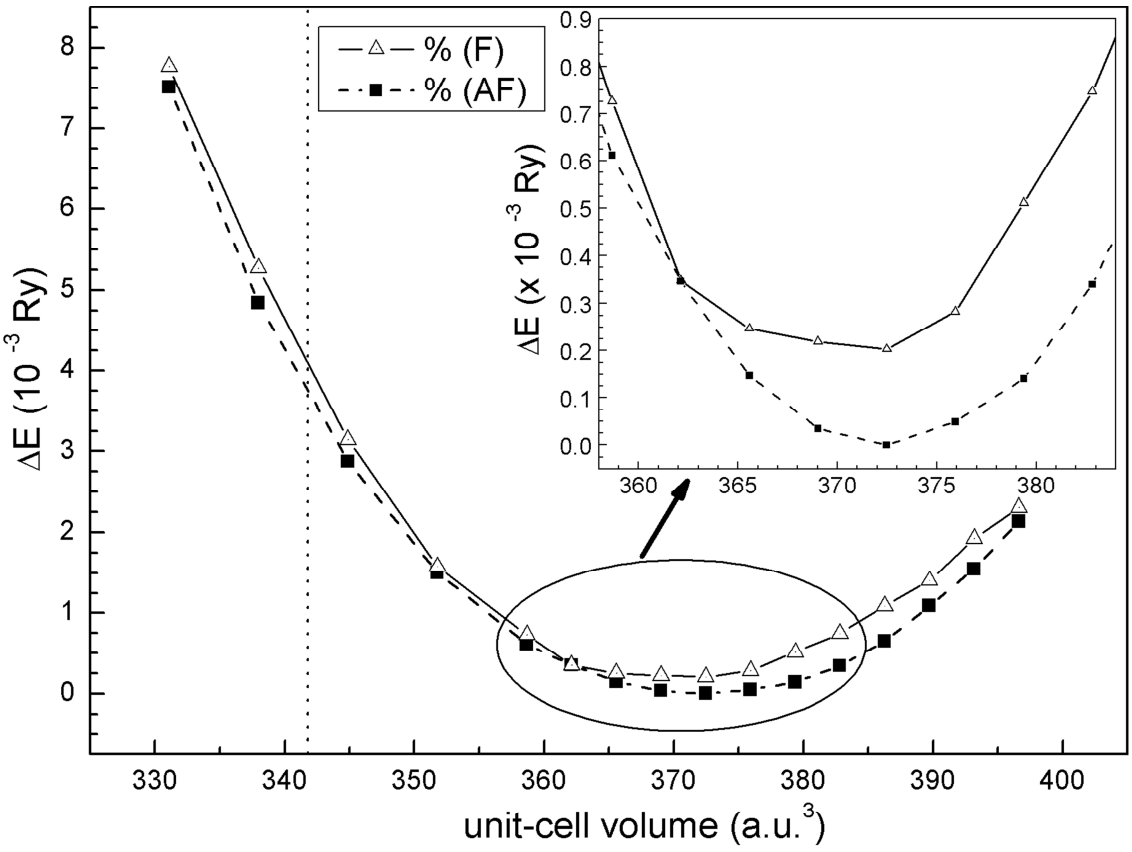

Fig. 10: Relative total energy as a function of the unit cell volume for ferromagnetic and anti-ferromagnetic NdAg. The vertical dotted line represents the experimental volume. [taken from Ref. 41]

The results of calculations for the total energy are shown in Fig. 10 as a function of the unit cell volume for the ferro-magnetic and anti-ferromagnetic couplings, and, as can be seen, the minimum of the energy in each case occurs at cell volumes around 8% larger than the experimental volumes, and the difference in energy between the ferromagnetic and anti-ferromagnetic cases of NdAg is very small, of the order of 10^{-4} Ry at the minimum of the curves. It was, then concluded that NdAg compound order anti-ferromagnetically and that the $(\pi,\pi,0)$ magnetic structure is not very stable.

Summary and Conclusions

In this review it was shown as to how useful PAC spectroscopy can be to investigate magnetic materials in an atomic scale. The emphasis was on the use of ^{140}Ce probe to investigate rare-earth based magnetic compounds. It has been shown that PAC can distinguish between two mechanisms of exchange in rare-earth compounds by measuring the polarization of *s*-conduction electrons, the RKKY coupling and the direct *d-d* coupling. It was also shown that PAC spectroscopy is able to measure the magnetic hyperfine field at different sites in the same compound.

References

[1] G.N. Rao: Hyperfine Interact. Vol. 7 (1979), p. 141

[2] P. Raghavan and R.S. Raghavan: Hyperfine interact. Vol. 24-26 (1985), p. 855

[3] S. Blügel, H.Akai, R.Zeller and P.H.Dederichs: Phys. Rev. B Vol. 35 (1987) p. 3271

[4] P. Novak: *New notes about hyperfine fields calculations*, on http://www.wien2k.at/reg_user/textbooks/Bhf_3.ps.

[5] A. Abragam and B.Bleaney: *Electron Paramagnetic Resonance of Transition Ions* (Clarendon Press, Oxford, 1970)

[6] M. A. Ruderman and C. Kittel: Phys. Rev. Vol. 96 (1954), p. 99

[7] T. Kasuya: Prog. Theor. Phys. Vol. 16 (1956) p. 45

[8] K. Yosida: Phys. Rev. Vol. 106 (1957) p. 893

[9] I. A. Campbell: J. Phys. F: Met. Phys. Vol. 2 (1972) p. L47

[10] G. Schatz and A. Weidinger: *Nuclear Condensed Matter Physics* (John Wiley & Sons, England 1996)

[11] A. W. Carbonari, W. Pendl Jr., R. N. Attili and R. N. Saxena: Hyperfine Interact. Vol. 80 (1993), p. 971

[12] A. W. Carbonari, R. N. Saxena, W. Pendl Jr., J. Mestnik-Filho, R. N. Attili, M. Olzon-Dionysio and S. D. de Souza: J. Magn. Magn. Mat. Vol. 163 (1996) p. 313

[13] M. Forker, R. Müsseler, S. C. Bedi, M. Olzon-Dionysio and S. D. de Souza: Phys. Rev. B. Vol. 71 (2005) p. 094404

[14] A. L. Lapolli, R. N. Saxena, J. Mestnik-Filho, D. M. T. Leite and A. W. Carbonari: J. Appl. Phys. Vol. 101 (2007) p. 09D510

[15] A. W. Carbonari, A. L. Lapolli, R. N. Saxena and J. Mestnik-Filho: Hyperfine Interact. Vol. 176 (2007), p. 101

[16] P. Hohenbeg and W. Kohn: Phys. Rev. Vol. 136 (1964) p. B864

[17] W. Kohn and L. J. Sham: Phys. Rev. Vol. 140 (1965) p. A1133

[18] S. Cottenier: *Density Functional Theory and the family of (L)APW-methods: a step-by-step introduction* (Instituut voor Kernen Stralingsfysica, K.U.Leuven, Belgium, 2002)

[19] David J. Singh: *Plane waves, pseudopotentials and the LAPW method* (Kluwer Academic, Boston, USA 1994)

[20] P. Blaha, K. Schwarz, G. K. H. Madsen, D. Kvasnika and J.Luitz: *WIEN2k An Augmented Plane Wave + Local Orbitals Program for Calculating Crystal Properties* (Karlheinz Schwarz, Techn. Universität Wien, Austria, 2001)

[21] A. W. Carbonari, J. Mestnik-Filho, R. N. Saxena and M. V. Lalic: Phys. Rev. B Vol. 69 (2004) p. 144425.

[22] M. V. Lalic, J. Mestnik-Filho, A. W. Carbonari and R. N. Saxena: J. Phys.: Condens. Matter Vol. 16 (2004) p. 6685

[23] A. W. Carbonari, J. Mestnik-Filho, R. N. Saxena and H. Saitovitch: Hyperfine Interact. Vol. 133 (2001), p. 77

[24] M. V. Lali'c, J. Mestnik-Filho, A. W. Carbonari, R. N. Saxena, H. Haas: Phys. Rev. B Vol. 65 (2001) p. 054405

[25] D. Torumba, V. Vanhoof, M. Rots, S. Cottenier: Phys. Rev. B Vol. 74 (2006) p. 014409

[26] D. Torumba, P. Novak, S. Cottenier: Phys. Rev. B Vol. 77 (2008) p. 155101

[27] J. Mestnik-Filho, L. F. D. Pereira, A. W. Carbonari: Hyperfine Interact. Vol. 176 (2007) p. 119

[28] P.W. Anderson: Phys. Rev. Vol. 124 (1961) p. 41

[29] Y. Koi, A. Tsujimura and T. Hihara: J. Phys. Soc. Japan Vol. 19 (1964) p. 1493

[30] V. Jaccarino, L. R. Walker and G. K. Wertheim: Phys. Rev. Lett. Vol. 13 (1964) p. 752

[31] G. G. Low: Phys. Lett. Vol. 21 (1966) p. 497

[32] D. A. Shirley, S. S. Rosenblum and E. Matthias: Phys. Rev. Vol. 176 (1968) p. 363

[33] I. A. Campbell: J. Phys. C: Solid State Phys. Vol. 3 (1970) p. 2151

[34] J. Friedel: Nuovo Cim. Vol. 7 (1958) p. 287

[35] G. Pramila and L. Grodzins, in: Hyperfine Structure and Nuclear Radiation, edited by E. Matthias and D. A. Shirley, p. 478, North-Holland, 1968

[36] H. Bernas and H. Gabriel: Phys. Rev. B Vol. 7 (1973) p. 468

[37] T. A. Thiel, E. Gerdau, M. Böttcher and G. Netz: Hyperfine Interact. Vol. 9 (1981) p. 459

[38] T. A. Thiel, E. Gerdau, B. Scharnberg and M. Böttcher: Hyperfine Interact. Vol. 14 (1983) p. 347

[39] E. Wäckelgard, E. Karlsson, B. Lindgren, A. Mayer and Z. Hrynkiewicz: Hypefine Interact. Vol. 51 (1989) p. 853

[40] A. W. Carbonari, F. H. M. Cavalcante, L. F. D. Pereira, G. A. Cabrera-Pasca, J. Mestnik-Filho and R. N. Saxena: J. Magn. Magn. Mater. Vol. 320 (2008) p. e478

[41] F. H. M. Cavalcante, L. F. D. Pereira , A. W. Carbonari, J. Mestnik-Filho and R. N. Saxena: submitted to Journal of Magnetism and Magnetic Materials (2009)

Defects and Diffusion Studied Using PAC Spectroscopy
doi:10.4028/www.scientific.net/DDF.311

Impurities in Magnetic Materials Studied by PAC Spectroscopy
doi:10.4028/www.scientific.net/DDF.311.39